Energy and Water Balance at Soil–Air Interface in a Sahelian Region

Minwei Qian[1,2,4], N. Loglisci[1], C. Cassardo[1], A. Longhetto[1,4], C. Giraud[3]

[1]*Department of General Physics, University of Turin, Italy*

[2]*Institute of Atmospheric Physics, Chinese Academy of Sciences, Beijing* 100029,

[3]*Institute of Cosmo–Geophysics, National Research Council (CNR), Turin, Italy*

[4]*ICSC–World Laboratory–Lausanne–Switzerland*

(Received September 1, 2000)

ABSTRACT

The aim of this work is an improvement of the parameterization of the soil moisture in the scheme of the Land Surface Process Model (LSPM) for applications over desert areas. In fact, in very dry conditions, the water vapour flux plays an important role in the evaporation processes and influences the underground profiles of humidity and temperature. The improved version of soil moisture parameterization in the LSPM scheme has been checked by using the data taken from the database of the field experiment HAPEX–Sahel (Hydrology–Atmosphere Pilot Experiment in the Sahel, 1990–1992). Model simulations refer to three different stations located in Niger (Fallow, Millet and Tiger sites) where input data for LSPM and observations were simultaneously available. The results of simulations, taking into account the water vapour flux in the soil model LSPM, seem to compare better with the observed behaviour of soil moisture and turbulent heat fluxes than those overlooking the water vapour flux, confirming the great importance of the water vapour in such dry conditions.

Key words: Drought, Heavy rain, Water vapour, Soil moisture, Evaporation, LSPM, SVAT, HAPEX, Sahel, Niger

1. Introduction

Model simulation of soil physical properties is very important for climate studies because of the role they play in different interaction processes with the atmosphere. One of the most widespread studies is the implementation of soil models in General Circulation Models (GCMs); previous studies showed, in fact, that climate simulations are sensitive to the parameterization of the energy and mass fluxes at the land surface (Viterbo, 1995; Beljiaars et al., 1996; Dolman et al., 1997). A large number of models have been developed to describe the surface fluxes of heat, water and momentum; they are called SVAT (Soil Vegetation Atmosphere Transfer) schemes. The LSPM scheme (Cassardo et al., 1995) is one of these models.

Land surface not only plays a very important role in influencing regional and global climate, but it is also strategic for the agriculture, especially in dry and desert areas. Because of the strong sunlight radiation and of the high hydraulic conductivity typical for the sandy regions, the land surface moisture in dry and desert areas can change dramatically in very short time, which is tremendously important for the local crops (and for the food supply to the local population and cattle).

Because dry lands occupy a large part of the entire land coverage and one quarter of the world's population inhabit dry lands and depend on these areas for their livelihood (UNEP,

1992), it becomes very important to make the soil models able to simulate such dry conditions. In order to do this, it could be helpful to include the water vapour in the computation of the water flux inside the model (Niu et al., 1997). In fact, it is just in these extreme situations, such as dry soils, that water vapour flux starts playing an important role in the water flux balance; leaving it out of account would bring about large errors in the model estimates of surface evaporation. In this paper, three HAPEX–Sahel (Hydrological and Atmospheric Pilot EXperiment in the Sahel, Goutorbe J.P. et al., 1993; Prince et al., 1995) observation sites in Niger have been selected for studying the underground water vapour contribution to the surface water budget. They are called Fallow, Millet and Tiger sites (Table 1).

2. Description of the selected region: the Sahel and the site of HAPEX–Sahel experiment

The region analysed in this study is located in the Sahel (Africa). The Sahel occupies a narrow zone, forming a strip about 400–600 km wide, bounded on the North by the Sahara and on the South by the Sudanian vegetation zone (Fig. 1). It stretches nearly 6000 km across the entire African continent.

The Sahel climate (Nicholson, 2000) is characterized by a single, short, annual rainy season associated with the Northward movement of the Inter Tropical Convergence Zone (ITCZ).

Despite of this severe climate, the Sahel is an area extensively exploited by the humans; thus, much of the landscape of the Southern and more favourable mid–Sahel consist of fields and extensive areas of fallow bushland in various stages of regrowth.

An area belonging to the Nigerian Sahel, of $1° \times 1°$ (latitude 2°–3° East and longitude 13°–14° North, corresponding to a surface of almost 100×100 km^2) was selected in

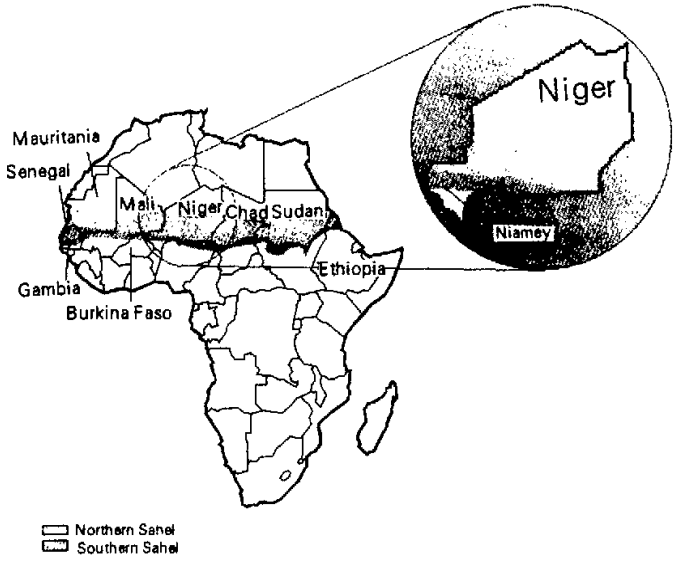

Fig. 1. The selected region: the Sahel in Niger near Niamey (the capital city).

1990–1992 for the HAPEX–Sahel field experiment. All the three sites mentioned before (Section 1) are located in this area (Table 1). Niamey, capital city of Niger, is in this area too.

Table 1. Coordinates of the three selected sites

Site	Latitude	Longitude
Fallow	13.244°N	2.244°E
Millet	13.241°N	2.999°E
Tiger	13.198°N	2.239°E

3. Description of the LSPM–SVAT scheme

The Land Surface Process Model (LSPM) has been developed by our groups (Turin University, Italy, and Institute of Atmospheric Physics of Beijing, China) in the frame of the World Laboratory Project Land 2 (Cassardo et al., 1995), and tested in Ruti et al., (1997) and in Cassardo et al., (1998). LSPM is a typical SVAT scheme developed to be used both as a "stand–alone" model (in this case, a set of specific routines for the calculation of the input data is provided) and as the surface boundary subroutine of an atmospheric circulation model (in this case, all input data are taken by the atmospheric model itself).

In this work LSPM is used in its stand–alone version, so the input data required are: air temperature, atmospheric pressure, specific or relative humidity, solar incoming radiation or cloudiness, horizontal wind speed components, rate of precipitation.

The schematic spatial structure of LSPM includes three main zones: the atmospheric layer above the vegetation (extending from a reference height to the vegetation canopy level), the vegetation layer (extending downward to the soil), and the soil layer. The hierarchy of the model allows a separation among soil, canopy and atmospheric layers. In the atmospheric layer, all output variables are calculated as weighted averages between atmospheric and canopy components. The canopy is considered as an uniform layer (big–leaf) characterized by the following parameters: vegetation cover, height, leaf area index (LAI), albedo, minimum stomatal resistance, leaf dimension, emissivity and root depth. Soil temperature and moisture are calculated using multi–layer schemes whose main parameters are: thermal conductivity, hydraulic conductivity, soil porosity, permanent wilting point, dry volumetric heat capacity, soil surface albedo and emissivity. The user can select a variable number of soil layers. Each flux is partitioned according to the vegetation and snow fractional covers. The model includes two subroutines for the long–wave and short–wave incoming radiation calculation (if not any observed radiation is available, the cloud coverage data is needed). The turbulent heat, water vapour and momentum fluxes are calculated by using the " analogue electric" scheme, in which the flux is expressed as a ratio between a generalized gradient (of temperature or moisture) and " resistances". LSPM can provide the values of each component of thermal and hydrological budgets in the soil, of the water balance in the planetary boundary layer and atmospheric turbulent fluxes.

The reader can refer to the previously quoted papers and to Loglisci et al., (2001) for a full description of the model and parameterizations used. Here, we will focus our attention on the parameterization of the water vapor flux.

4. Modifications of soil moisture equation including the water vapor flux

The soil moisture prognostic equation used in LSPM is

$$\frac{\partial \eta}{\partial t} = -\frac{\partial Q_z}{\partial z} + Q_{\eta so} - Q_{\eta si}, \tag{1}$$

where $Q_{\eta so}$ (s^{-1}) and $Q_{\eta si}$ (s^{-1}) represent the source and sink terms, respectively. η ($m^3 m^{-3}$) is the soil volumetric water content and Q_z ($m\,s^{-1}$) the soil total water flux. The soil water flux was calculated by LSPM as liquid water flux according to the equation

$$Q_z = -D_{l\eta}\frac{\partial \eta}{\partial z} - K_\eta, \tag{2}$$

where $D_{l\eta}$ ($m^2 s^{-1}$) is the hydraulic diffusivity and K_η (ms^{-1}) the hydraulic conductivity. These two variables are expressed by using the Clapp and Horneberger (1978) formulation (hereafter referred as CH78) as

$$D_\eta = K_\eta \frac{\partial \psi}{\partial q}, \tag{3}$$

$$K_\eta = K_s q^{2b+3}, \tag{4}$$

where $\psi(m)$ is the moisture (matrix) potential, given by

$$\psi_\eta = \psi_s q^{-b}. \tag{5}$$

In equations (3)–(5), the saturated values K_s and ψ_s (together with the experimental parameter b, related to the soil texture) are tabulated for different soil according to the tables of CH78 or Cosby et al. (1982).

In this work, the underground water vapor flux has been added into the equation (2). In fact, Niu et al. (1997) demonstrated that, when the volumetric soil content is lower than 0.06 m^3 / m^3, the underground water vapor begins to play an important role in the computation of the water flux in the soil. As evaporation and heat fluxes are proportional to the soil moisture content and to the soil temperature gradient, the inclusion of the water vapor phase, in addition to the liquid water phase, can become very important in dry conditions.

The total water flux into soil can then be expressed as the sum of liquid water and water vapor in the following way

$$Q_z = -(D_{l\eta} + D_{v\eta})\frac{\partial \eta}{\partial z} - K_\eta - D_{vT}\frac{\partial T}{\partial z}, \tag{6}$$

where the water vapor hydraulic diffusivity $D_{v\eta}$ ($m^2 s^{-1}$) and the water vapour thermal diffusivity D_{vT} ($m^2 K^{-1} s^{-1}$) can be expressed as

$$D_{v\eta} = -\frac{D_w \tau (1-q)\rho_v g \psi_s b}{\rho_w R_w T q^{b+1}}, \tag{7}$$

$$D_{vT} = -\frac{D_w \tau \eta_s (1-q)\rho_v}{\rho_w}\left[\frac{1}{T} + \frac{g\psi}{R_w T^2} - \frac{17.269 * 273.3}{(T-35.86)^2}\right]. \tag{8}$$

In these formulations, τ is the dimensionless soil tortuosity (connected to the size of sand grains), $q = \eta / \eta_s$ the relative soil moisture, η_s the soil porosity, b the CH78 exponent, ρ_w the water density, T the soil temperature, $R_w = 287$ J / kg K the water vapour constant, ρ_v

the water vapor density, parameterized as

$$\rho_v = \frac{e_s^*(T)\exp(\frac{g\psi}{R_v T})}{R_v T}, \tag{9}$$

where $e_s^*(T)$ is the saturated vapour pressure over the free water surface at the local averaged soil temperature T and g is the acceleration of gravity; finally D_w (m^2s^{-1}) is the water vapour diffusivity, expressed by

$$D_w = 2.3\times 10^{-5}(\frac{T}{273.16})^{1.75}. \tag{10}$$

Substituting equation (6) into equation (1), we can obtain the soil moisture equation currently used in LSPM, i.e.

$$\frac{\partial \eta}{\partial t} = \frac{\partial}{\partial z}(D_{l\eta} + D_{v\eta})\frac{\partial \eta}{\partial z} + \frac{\partial K_\eta}{\partial z} + \frac{\partial}{\partial z}(D_{vT}\frac{\partial T}{\partial z}) + Q_{\eta so} - Q_{\eta si}. \tag{11}$$

5. The LSPM initialization

The input data required by LSPM have been taken from the HAPEX–Sahel field experiment. As already mentioned in Section 3, LSPM needs the following data: air temperature, atmospheric pressure, precipitation rate, solar radiation or cloudiness, specific or relative humidity and horizontal wind components.

For all simulations, we have used 8 soil layers whose thickness was respectively 0.1, 0.2, 0.3, 0.4, 0.5, 0.6, 1.0, 1.5 m.

The entire dataset of the HAPEX–Sahel experiment consists of the observations referring to the period from middle of 1990 to late 1992. From this dataset we selected the data (including the input) of the period from 17 August 1992 to 6 October 1992 (the rainy season) during which the soil moisture was measured in the three sites mentioned in Sections 1 and 2.

6. The results

Among all outputs calculated by LSPM, we selected those allowing to make the comparison with the observed data of the following variables: soil moisture at different depths, net radiation, sensible and latent heat fluxes.

The following Subsections give a detailed account of the main results achieved in the three selected sites.

6.1 *The Fallow site*

From Fig. 2, which shows the observed soil moisture in Fallow site, it appears that, after the heavy rain period, the soil moisture responds very quickly to the precipitation even at the deepest two levels. For instance, on August 22 and 31 (see also Fig. 3), the daily averaged precipitation rate reached 37 mm / day and 49 mm / day, respectively. Obviously, the soil moistures at 10 cm and 20 cm got wet immediately, while the soil moisture at 120 cm took only 1 day to feel the surface water maximum and that at 180 cm took about 2 or 3 days. This fact proves that the soil in this region has very high hydraulic conductivity. According to our

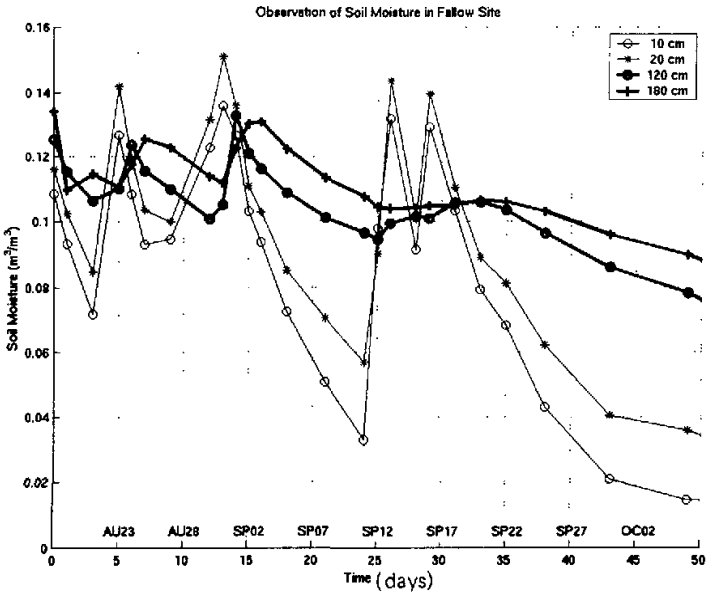

Fig. 2. Observed soil moisture in Fallow site, at 10 cm, 20 cm, 120 cm and 180 cm below the surface, respectively.

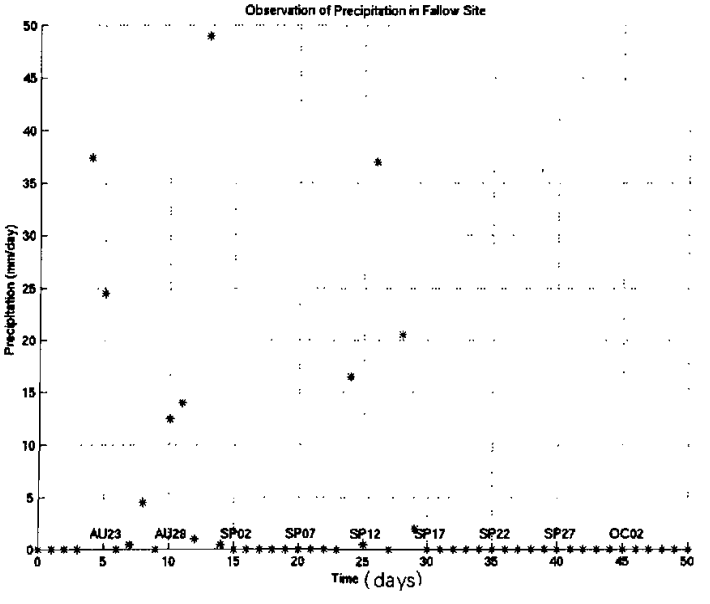

Fig. 3. Daily averaged precipitation rate (mm / day) in Fallow site.

experiences, it is quite unlikely that sandy soil parameters of CH78 can bring about such a high conductivity. In fact, LSPM failed when sandy soil parameters of CH78 were used in LSPM to simulate the soil moisture profile, as shown in Figs. 4a, 4b, 4c, 4d referring to LSPM simulation of soil moisture with the sandy soil parameters of CH78.

From Figs. 4a and 4b, referring to the first two layers, we can see that the simulation of the soil moistures with soil parameters of CH78 greatly overestimates the observation by more than 0.05 m^3m^{-3}. The differences increase when soil becomes drier. Of course, simulations and observations are in phase since these soil layers are near the surface. However, when we look at Figs. 4c and 4d, not only the simulations overestimate the observations, but they are also out of phase. In Fig. 4c, the soil 120 cm below the surface took almost 10 days to respond the rainfall instead of 1 day, as shown by the observation (Fig. 2). Because of the failure of such a simulation, we tried to use for the simulation new sandy soil parameters measured in Grugliasco (Turin, Italy), where a hill rich of pure sandy land coming from an ancient glacial deposit is present. The Grugliasco sand is characterized by an extremely high hydraulic conductivity. We call it " pure sand". Table 2 shows the new soil parameters, against the corresponding ones of CH78.

According to the parameterization of hydraulic conductivity $K_i = K_{sat}(q_i^{2b+3})$, under moderate soil moisture condition $[q_i = (\frac{\theta_i}{\theta_{sat}} \approx 0.5]$, the hydraulic conductivity of the pure

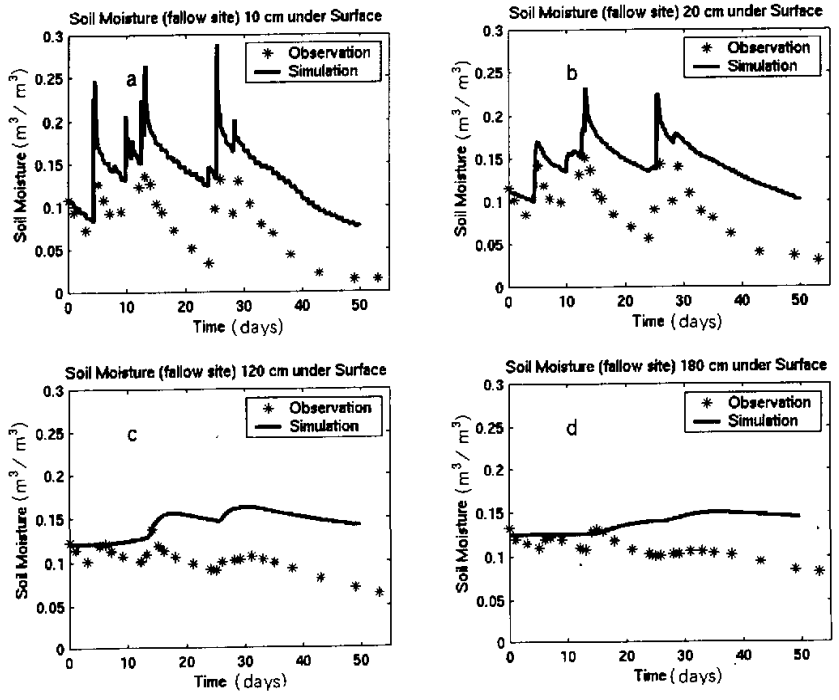

Fig. 4(a–d). Observed versus simulated soil moisture in Fallow site, at 10, 20, 120 and 180 cm below the surface, with soil parameters of CH78.

sand is about 5 times larger than that of CH78, and under dry soil moisture condition [$q_l = (\frac{\theta_l}{\theta_{sat}} \approx 0.25$], the hydraulic conductivity of the pure sand is about 100 times larger than that of CH78. By using these sandy soil parameters of the pure sand, we simulated the soil moisture again in Fallow site. Figs. 5a, 5b, 5c and 5d show the results.

Table 2. Sandy soil parameters in Grugliasco compared with those of CH78

	Saturated volumetric water content θ_{sat} ($m^3\ m^{-3}$)	Saturated water matrix potential Ψ_{sat} (m)	exponent b of $\Psi_l = \Psi_{sat}(\frac{\theta_l}{\theta_{sat}})^{-b}$
CH78 sand	0.395	0.121	4.05
"Pure sand"	0.40	0.180	2.0

In this case, the soil moistures look well simulated. The simulation values not only show a good agreement with the observations, but they are also in phase at all levels underground. A noticeable feature in Fig. 5a is that the simulated soil moisture (at 10 cm under the surface) shows much higher values during the short raining period. This is not necessarily a fault of simulation. On the contrary, this is because the observation of soil moisture was made after

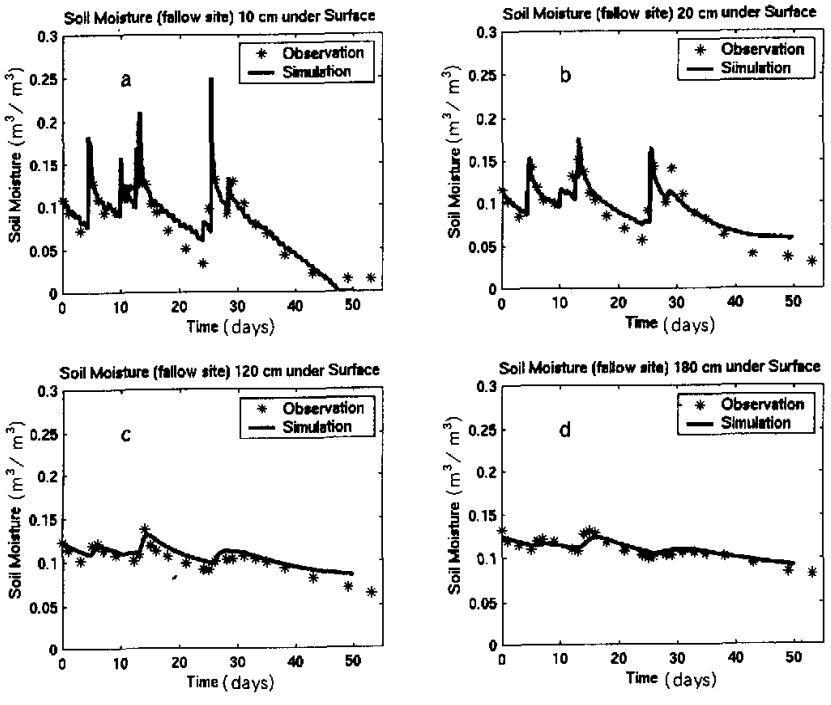

Fig. 5(a–d). Observed versus simulated soil moisture in Fallow site, at 10, 20, 120 and 180 cm below the surface with observed "pure sand" soil parameters in Grugliasco, Italy, without considering the contribution of underground water vapor to the surface water budget.

rain stopped. Due to the very high hydraulic conductivity, the soil moisture near the surface decreases very quickly. A lot of water near the surface has infiltrated into deeper levels before the observation was made.

Even if the LSPM simulation shows a sharp improvement when the observed soil parameters of the pure sand are used, there are still some problems in Figs. 5a and 5b. From Fig. 5a, we can find that, at the end of simulation, the first layer of soil moisture almost goes to zero rather than to the observed value of 0.02 m^3m^{-3}. When the first layer of soil moisture θ_1 becomes very dry, surface resistance that accounts for water vapor transfer between the soil and surface (which in turn is a function of θ_1) becomes very high. This reduces the surface evaporation over bare soil surface (Gash et al., 1991; Kabat et al., 1997) and hampers the deep soil moisture from going up to the surface. In this case, only the transpiration is left. In fact, from Fig. 5b, we can see that at the end of simulation the soil moisture at 20 cm below the surface slightly overestimated the observation. These problems are due to the fact that the model was not able to extract water from dry soil, after evaporation of most of surface liquid water, because the scheme of underground water vapor was not activated. When this scheme is activated, we got Figs. 6a, 6b, 6c and 6d.

By comparing Figs. 6a and 6b with Figs. 5a and 5b, we can clearly appraise the improvement of the simulation after activation of the underground water vapor scheme.

With the observed " pure sandy soil" parameters, not only soil moistures, but also soil temperature, surface heat fluxes and net radiation are well simulated. Figs. 7a, 7b, 7c and 7d show observed versus simulated soil temperature at 10 cm under the surface, and surface

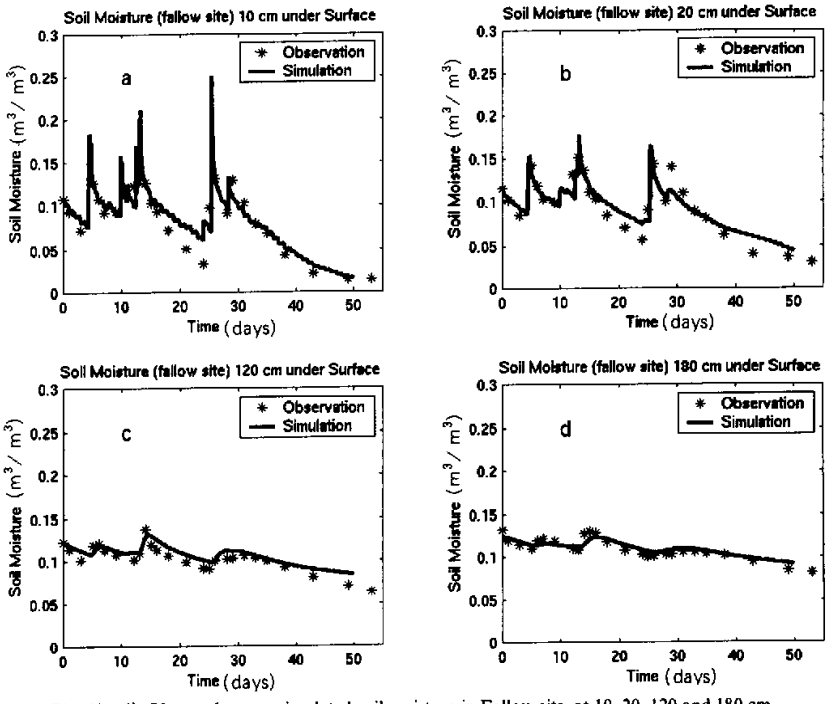

Fig. 6(a–d). Observed versus simulated soil moisture in Fallow site, at 10, 20, 120 and 180 cm below the surface, with observed " pure sand" soil parameters in Grugliasco, Italy and with considering the contribution of underground water vapour to the surface water budget.

sensible heat flux, latent heat flux and net radiation respectively.

Generally speaking, soil temperature is well simulated. Only during some short period, its simulation underestimates the observation.

As far as sensible heat flux, latent heat flux and net radiation flux are concerned, continuous observation could hardly be available in Fallow site, because the instruments used by HAPEX–Sahel exhibited some problems to work properly when it rained. From the few days of observations, we can see that the observed sensible heat flux is quite small. Generally speaking, the daily averaged sensible heat flux is about 30 Wm^{-2}. The observed latent flux is 3 times larger than the observed sensible heat flux, which demonstrates the high evaporation in this region (Verhoef et al., 1999). Only after the raining season, when the soil becomes dry, the observed sensible heat flux starts increasing and the observed latent heat flux decreasing. They become comparable at the end of the considered observation period.

LSPM proves to be able to reproduce this phenomenon very well. The simulations meet the observations properly, when these last are available. Fig. 7c, more than the other three figures, seems to suggest that the simulated latent heat flux exceeds some time the observed one. Once again, this is only an apparent disagreement, due to the fact that the observed values are not as regular and continuous in time as simulation is.

6.2 *The Millet and Tiger sites*

With the same soil parameters used for Fallow site and the scheme of underground water vapour set on, LSPM was also applied to Millet and Tiger sites. Figs. 8a, 8b, 8c and 8d show

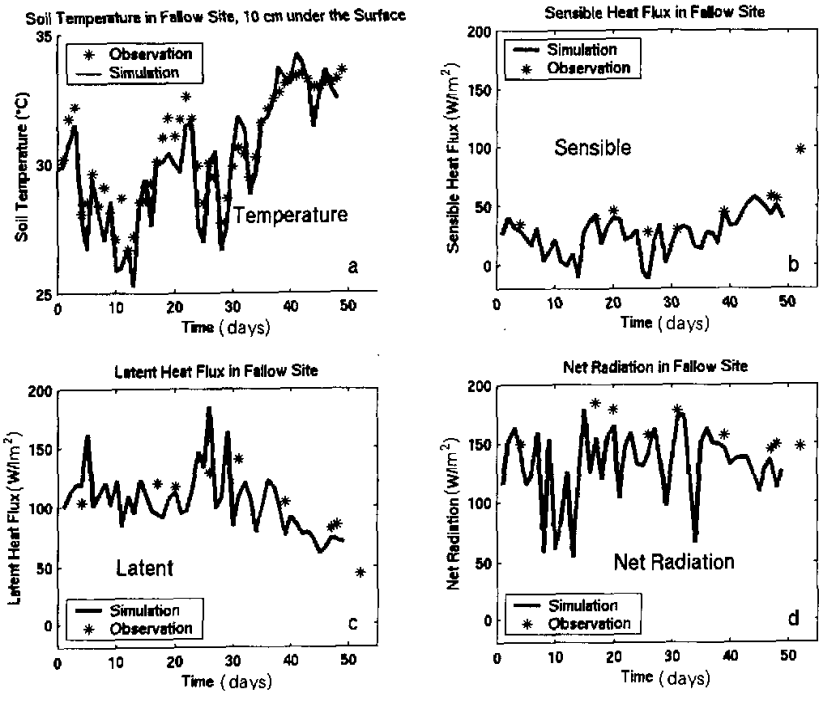

Fig. 7 (a) Observed versus simulated soil temperature at 10 cm under surface; (b) Observed versus simulated sensible heat flux; (c) Observed versus simulated latent heat flux; (d) Observed versus simulated net radiation.

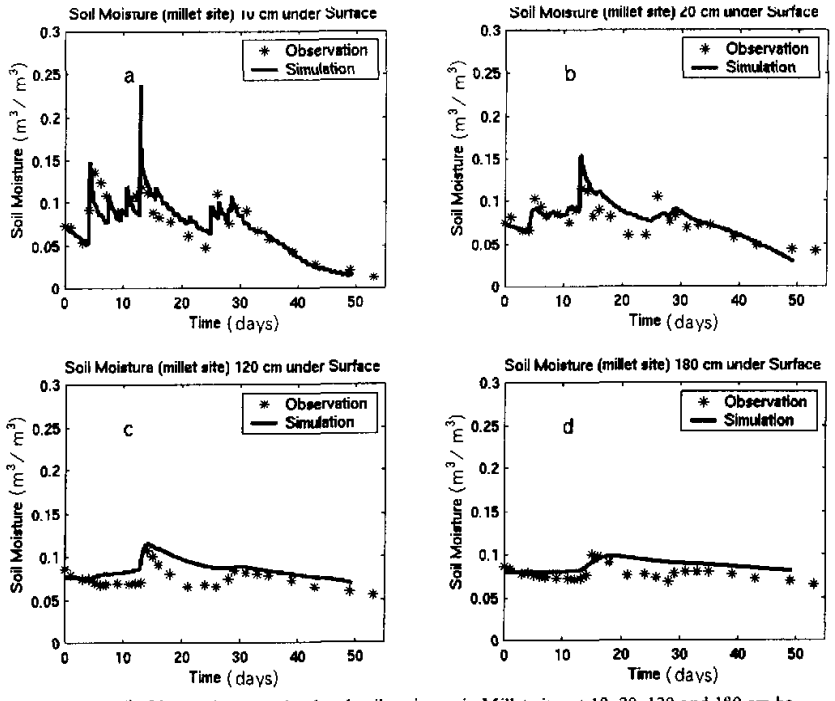

Fig. 8 (a–d). Observed versus simulated soil moisture in Millet site, at 10, 20, 120 and 180 cm below the surface, with observed " pure sand" soil parameters in Grugliasco, Italy and with considering the contribution of underground water vapour to the surface water budget.

the simulation of soil moisture in Millet site. Simulation of other physical quantities were not carried out here, because of shortage and randomness of relevant observations.

Generally speaking, the simulation in Millet site shows good agreement with the observation at all levels. The careful readers might find that the simulation at the deepest levels Figs. 8c and 8d did not follow the observation as precisely as it did in Fallow site Figs. 6c and 6d. Nevertheless, this result still keeps good enough for practical applications.

The simulation of soil moisture in Tiger site, on the contrary, shows a different feature.

The agreement of simulation with observation at the levels near the surface is not so bad (Figs. 9a and 9b) except for the first three days. But the simulation at the deepest levels Figs. 9c and 9d is unacceptable. What we could not understand is why the observation values at deep levels in Tiger site keep very high after the rain stopped. They almost reached and held the saturated value. Probably, the water table level here is quite high. If this is true, the observation would refer to a different phenomenology from the one simulated by our model.

7. Conclusions

According to both the observation and model simulation of soil moisture in Nigerian Sahel, it proves that the hydraulic conductivity in the studied sites is higher than one prescribed by CH78 for sand soil. Because of the high hydraulic conductivity, the surface soil moisture becomes very dry shortly after rain stops. Under this circumstance, it is necessary to take account of the underground water vapour contribution to the surface water budget. Our

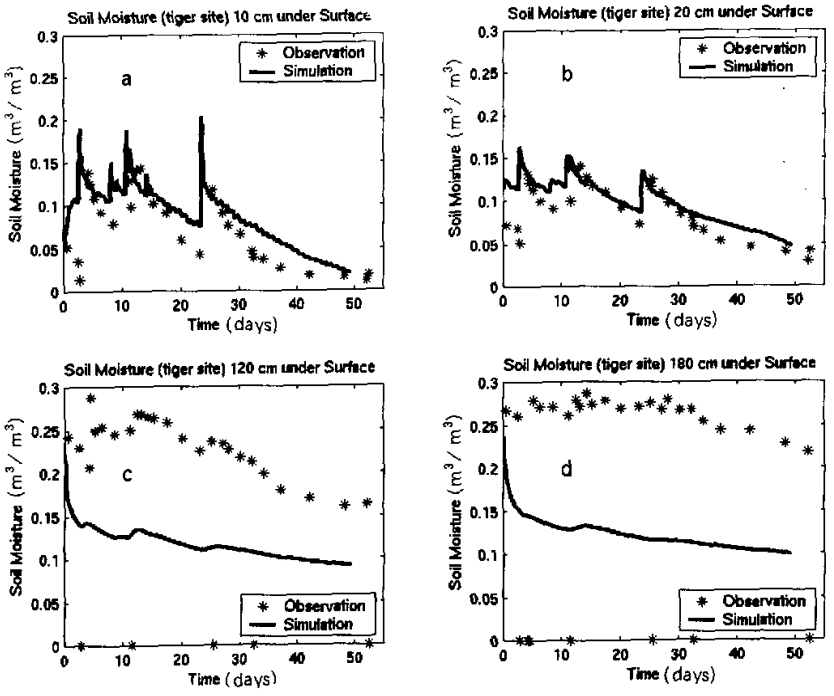

Fig. 9 (a–d). Observed versus simulated soil moisture in Tiger site, at 10, 20, 120 and 180 cm below the Surface, with observed " pure sand" soil parameters in Grugliasco, Italy and considering the contribution of underground water vapour to the surface water budget.

Land Surface Process Model (LSPM) has been upgraded with this scheme to simulation soil moisture under this extreme condition. The simulation results show great improvement with this scheme.

The authors are grateful to the HAPEX–Sahel Information System, which let the database available in Internet. We thank Dr. P. Viterbo as well for his help in the search of references and for his suggestions and Dr. G. Y. Niu for permitting the use of his model. We are indebted with Dr. Stefano Ferraris of the DIPARTIMENTO DI ECONOMIA ED INGEGNERIA AGRARIA FORESTALE ED AMBIENTALE (DEIAFA) of the University of Turin (Italy) for providing us the observed soil parameters relative to Grugliasco sandy hill and for interesting discussions.

REFERENCES

Beljiaars A.C.M., P. Viterbo, M.J. Miller, and A.K. Betts, 1996: The anomalous rainfall over the United States during July 1993: sensitivity to land surface parameterization and soil moisture anomalies. *Mon. Wea. Rev.*, **124**, 362–383.

Cassardo C., E. Carena, and A. Longhetto, 1998: Validation and sensitivity tests on improved parameterizations of a Land Surface Process Model (LSPM) in the Po Valley, Il Nuovo Cimento 21C n.2, 87–121.

Cassardo C., J. J. Ji, and A. Longhetto, 1995: A study of the performance of a land surface process model (LSPM). *Boundary–Layer Meteorology*, **72**, 87–121.

Clapp R. B., and G. M. Horneberger, 1978: Empirical Equations for Some Hydraulic Properties, *Water Resources Research*, **14**, 601–604.

Cosby B. J., G. M. Horneberger, R. B. Clapp, and T. R. Ginn, 1984: A statistical exploration of the relationships of soil moisture characteristics to the physical properties of soils, *Water Resources Research*,20 n,6, 682–690.

Dolman A.J., et al., 1997: The role of the land surface in Sahelian climate: HAPEX–Sahel results and future research needs. *J. Hydrol.*, Amsterdam, 188–189, 1067–1079.

Gash J.H.C., J.S. Wallace, C.R. Lloyd, A.J. Dolman, M.V.K. Sivakumar, and C. Renard, 1991: Measurements of evaporation from fallow Sahelian savannah at the start of the dry season. *Quart. J. Royal Meteorological Society*, **117**, 749–760.

Goutorbe J.P., T. Lebel, A. Tinga, P. Bessemoulin, J. Brouwer, A.J. Dolman, E.T. Engman, J.H.C. Gash, M. Hoepffner, P. Kabat, Y.H. Kerr, B. Monteny, S. Prince, F. Said, P. Sellers, and J.S. Wallace, 1993: HAPEX–Sahel a large scale study of land–atmosphere interaction in the semi–arid tropics. *Ann. Geophys.* **12**, 53–64.

Huntingford C., S.J. Allen, and R.J. Harding, 1995: An inter–comparison of single and dual–source vegetation–atmosphere transfer models applied to transpiration from Sahelian Savannah, *Boundary–Layer Meteorology*, **74**, 397–418.

Kabat P., A.J. Dolman, and J.A. Elbers, 1997: Evaporation, sensible heat and surface conductance of fallow savanna and patterned woodland in the Sahel. *J. Hydrol.*, Amsterdam, 188–189, 494–515.

Loglisci N., G.P. Balsamo, C. Cassardo, and M.W. Qian, 2001: A technical description of the Land Surface Process Model (LSPM), version 2000, Internal report C.S.I. (Sala Situazione Rischi Naturali, C.so Unione Sovietica, 216–10134 Torino, Italy, loglisci@ph.unito.it).

Niu G.Y., S.F. Sun, and Z.X. Hong, 1997: Water and heat transport in the desert soil and atmospheric boundary layer in western China. *Boundary–Layer Meteorology*, **85**, 179–195.

Nicholson S, 2000: Land Surface Processes and Sahel climate. *Reviews of Geophysics*, **38**, 117–139.

Prince S.D., Y.H. Kerr, J.P. Goutorbe, T. Lebel, A. Tinga, J. Brouwer, A.J. Dolman, E.T. Engman, J.H.C. Gash, M. Hoepffner, P. Kabat, B. Molteny, F. Said, P. Sellers, and J. Wallace, 1995: 'Geographical Biological and Remote Sensing aspects of the Hydrologic Atmosphere Pilot Experiment in the Sahel (HAPEX–Sahel), *Remote Sensing Environment*, **51**, 215–234.

Ruti P.M., C. Cassardo, C. Cacciamani, T. Paccagnella, A. Longhetto, and A. Bargagli, 1997: Inter–comparison between BATS and LSPM surface schemes, using point micrometeorological data set. *Beitr. Phys. Atm.*, **70**, 201–220.

Verhoef A., S. J. Allen, and C.R. Lloyd, 1999: Seasonal variation of surface energy balance over two Sahelian surfaces. *International Journal of Climatology*, **19**, 1267–1277.

UNEP, 1992: World Atlas of Desertification. *Pub. Edward Arnold*, UK.

Viterbo P., 1995: Initial values of soil water and the quality of the summer forecast. *ECMWF Newsletter*, **69**, 2–8.